

Solubility of the Ternary System $\text{LiCl} + \text{NH}_4\text{Cl} + \text{H}_2\text{O}$

Haitang Ouyang,[†] Dewen Zeng,^{*,†,‡} Hongyan Zhou,[†] Haijun Han,[†] and Yan Yao[†]

[†]Qinghai Institute of Salt Lakes, Chinese Academy of Sciences, Xining, 810007, P. R. China

[‡]College of Chemistry and Chemical Engineering, Central South University, Changsha, 410083, P. R. China

ABSTRACT: Solubility isotherms of the ternary system ($\text{LiCl} + \text{NH}_4\text{Cl} + \text{H}_2\text{O}$) were elaborately determined at $T = (273.15, 298.15, \text{ and } 323.15)$ K by an isothermal method. In the equilibrium phase diagram, there are two solubility branches at 273.15 K, corresponding to the solid phase $\text{LiCl} \cdot 2\text{H}_2\text{O}$ and NH_4Cl . The invariant point composition at 273.15 K is $w = 0.401$ for LiCl , $w = 0.024$ for NH_4Cl , and $w = 0.575$ for H_2O . However, there are three solubility branches at (298.15 and 323.15) K, corresponding to the solid phase $\text{LiCl} \cdot \text{H}_2\text{O}$, NH_4Cl , and a new found solid solution phase $(\text{NH}_4\text{Cl})_x(\text{LiCl} \cdot \text{H}_2\text{O})_{1-x}$. A Pitzer–Simonson–Clegg thermodynamic model was selected to represent the thermodynamic properties of this system. Thermodynamic consistence between our solubility data and water activity from other research groups shows that these concerned experimental data are reliable.

INTRODUCTION

Thermodynamic properties of the ternary system $\text{LiCl} + \text{NH}_4\text{Cl} + \text{H}_2\text{O}$, including its solid–liquid phase diagram, are of essential importance in the extraction of lithium chloride from natural salt brine containing mainly magnesium chloride and lithium chloride. As it is well-known, the economical separation of magnesium and lithium in magnesium-rich brine is a challenge for chemical engineers. An effective approach was proposed to precipitate Mg^{2+} into $\text{Mg}(\text{OH})_2$ by ammonium,¹ which can be reproduced by reacting CaO with NH_4Cl at high temperatures. After precipitation, the brine system converts from $\text{MgCl}_2 + \text{LiCl} + \text{H}_2\text{O}$ into $\text{NH}_4\text{Cl} + \text{LiCl} + \text{H}_2\text{O}$. Usually it is desirable to crystallize NH_4Cl from the solution by evaporation and then precipitate lithium as lithium carbonate. To prevent cocrystallization of LiCl with NH_4Cl , one needs knowledge of the phase diagram of the system $\text{LiCl} + \text{NH}_4\text{Cl} + \text{H}_2\text{O}$.

Up to now, some solubility isotherms^{2,3} measured for this system are doubtful. For instance, Wang et al.³ measured solubility isotherms of this system at $T = (273.15 \text{ and } 303.15)$ K and pointed out that equilibrium solid phase at 273.15 K is $\text{LiCl} \cdot \text{H}_2\text{O}$ but not $\text{LiCl} \cdot 2\text{H}_2\text{O}$. In fact, the latter should be the right one according to our previous critically evaluated result.⁴ Voskresenskaya's solubility data² at $T = 298.15$ K are somewhat scattered, and the wet solids' compositions were not reported for all equilibrium experiments. Whether the solubility data at 298.15 K are reliable is unknown at this stage.

In this paper, the solubility isotherms of the system ($\text{LiCl} + \text{NH}_4\text{Cl} + \text{H}_2\text{O}$) including the corresponding equilibrium solid phase have been elaborately determined at $T = (273.15, 298.15, \text{ and } 323.15)$ K, as well as the composition of the corresponding wet solid phases and dried solid phases.

Finally, an empirical Pitzer–Simonson–Clegg model was selected to simulate the properties of this system.

EXPERIMENTAL SECTION

Materials and Apparatus. Lithium chloride was prepared by neutralizing lithium carbonate (purity in mass fraction > 0.999 , Shanghai China-Lithium Industry Co. Ltd.) with hydrochloric

acid (G.R.). Ammonium chloride was analytical grade reagent (Tianjin Hengxing Industry Co. Ltd.). These salts were then purified twice by crystallization in each case with half salt recovery. Doubly distilled water ($S \leq 1.2 \cdot 10^{-4} \text{ S} \cdot \text{m}^{-1}$) and silver nitrate (purity in mass fraction > 0.999) were used in the experiment.

Solubility measurements were carried out in a thermostat (LAUDA E219, Germany) with a temperature stability of ± 0.01 K. The temperature was determined by means of a calibrated glass thermometer with an accuracy of ± 0.01 K. A Sartorius (CPA225D) balance was used for weighing with an error of ± 0.1 mg.

Experimental Procedures. Solid–liquid equilibrium experiments were carried out in a ground 250 cm^3 Erlenmeyer flask which was immersed in the glycol–water bath in the thermostat. Solution and solid in the flask were stirred with a magnetic stirrer outside the glycol–water bath. Each sample was stirred at a certain constant temperature for 72 h and then kept static for about 8 h. The sample of the saturated solution was then taken with a pipet covered with glass cloth as a filter and transferred to a weighed 30 cm^3 quartz bottle (1) and a weighed 25 cm^3 weighing bottle (2) with internal stoppers, respectively. The wet solid was transferred by glass scoop into a weighed 40 cm^3 glass-stoppered weighing bottle (3). Then, all of the rest of the solid and solution in the flask were taken out and separated by a filter crucible; the separated solid was washed rapidly by alcohol in a vacuum-filtration system and dried in a vacuum desiccator for about one hour. Then, the dried solid was taken into a weighed 40 cm^3 glass-stoppered weighing bottle (4). The solids and the solution were then analyzed according to the following procedures:

- Gradually evaporate the solution in bottle (1) in an oven and keep the dried salt at $T = 723$ K for about 2 h until all NH_4Cl has been decomposed thoroughly. Remove the

Special Issue: John M. Prausnitz Festschrift

Received: October 19, 2010

Accepted: January 10, 2011

Published: February 04, 2011

bottle into a desiccator, and cool to room temperatures, weighing the bottle with the sample; the difference is the amount of LiCl.

- (b) The total concentration of LiCl and NH₄Cl in the ternary system was determined by precipitating Cl⁻ ion in a bottle (2) with AgNO₃, as described in the literature.⁵ The difference with the previous procedure (a) is the amount of NH₄Cl.
- (c) The compositions of wet solid and dried solid were determined by analyzing the samples in bottle (3 and 4) as in the procedures (a and b).

Table 1. Solubility of the Ternary System LiCl + NH₄Cl + H₂O at 273.15 K

composition of solution ^a			composition of wet solid phase ^a			
LiCl	NH ₄ Cl	H ₂ O	LiCl	NH ₄ Cl	H ₂ O	solid phase ^b
0.4075	0	0.5925				A
0.4047	0.0098	0.5855	0.4610	0.0053	0.5337	A
0.4020	0.0224	0.5756	0.4703	0.0116	0.5181	A
0.4011	0.0241	0.5748	0.4595	0.0216	0.5189	A + B
0.4010	0.0242	0.5748	0.4049	0.0782	0.5169	A + B
0.4008	0.0243	0.5751	0.4323	0.0524	0.5153	A + B
0.3522	0.0276	0.6202	0.2838	0.2185	0.4977	B
0.2942	0.0310	0.6748	0.2257	0.2567	0.5176	B
0.1954	0.0636	0.7410	0.1555	0.2565	0.5880	B
0.1901	0.0662	0.7437	0.1491	0.2625	0.5884	B
0.1349	0.1015	0.7635	0.1099	0.2694	0.6207	B
0.1136	0.1179	0.7685	0.0776	0.3982	0.5242	B
0.0748	0.1522	0.7730	0.0561	0.3674	0.5765	B
0.0534	0.1739	0.7727	0.0434	0.3305	0.6261	B
0	0.2307	0.7693				B

^aThe mass fraction of the salt. ^bA = LiCl·2H₂O, B = NH₄Cl.

The type of solid phase in equilibrium with solution was determined by the Schreinemaker's method.

Accuracy Analysis. In each run of solubility experiments for the binary systems (LiCl + H₂O) and (NH₄Cl + H₂O), two parallel flasks were always used. Before each equilibrium experiment, the temperature of one flask with the sample solution was kept 5 K above and the other flask 5 K below the temperature of destination for about 4 h. Then, the flasks were moved to the thermostatic water bath at the equilibrium temperature. Solution analysis was made at a regular time interval. The difference in salt mass fraction between two subsequent samples decreased to 0.00015 after 56 h, compared with 0.0015 after 32 h. Thus, the equilibration time was taken to be 56 h for each run. For the ternary system, the equilibrium time was prolonged to 78 h.

Several gravimetric methods were compared with each other to determine the LiCl content. The influence of the NH₄Cl on the measurement of LiCl by gravimetric dehydration-method was systematically studied. Two parallel samples were taken from the same stock solution. In the analysis process, an appropriate amount of NH₄Cl was added to one of them, and it was found that the relative error between the two analyzed LiCl contents is about 0.06 %. Duplicate analysis of the same sample (solution and solids) gave maximal deviations of 0.08 %. Overall, the uncertainty of the experimental solubility results in this work can be reasonably evaluated to be less than 0.002 in mass fraction.

EXPERIMENTAL RESULTS AND DISCUSSION

The experimental solubility data at $T = (273.15, 298.15, \text{ and } 323.15)$ K are given in Tables 1 to 3 and plotted in Figures 1, 2, and 3, respectively.

The solid phases in equilibrium with saturated solutions are LiCl·2H₂O and NH₄Cl at $T = 273.15$ K. The invariant point composition at 273.15 K is $w = 0.401$ for LiCl, $w = 0.024$ for NH₄Cl, and $w = 0.575$ for H₂O. The saturation LiCl concentration in equilibrium with LiCl·2H₂O in the binary LiCl + H₂O system $w = 0.4075$ in this work agrees with our previous

Table 2. Solubility of the Ternary System LiCl + NH₄Cl + H₂O at 298.15 K

no.	composition of solution ^a			composition of wet solid phase ^a			composition of dried solid phase ^b			solid phase ^c
	LiCl	NH ₄ Cl	H ₂ O	LiCl	NH ₄ Cl	H ₂ O	LiCl	NH ₄ Cl	H ₂ O	
1	0.4573	0	0.5427							A
2	0.4511	0.0167	0.5322	0.4857	0.0143	0.5000				A
3	0.4441	0.0220	0.5339	0.4625	0.0547	0.4828	0.5546	0.2085	0.2369	S
4	0.4366	0.0277	0.5357	0.4313	0.0888	0.4799	0.3991	0.4289	0.1720	S
5	0.4138	0.0400	0.5462	0.3890	0.1599	0.4511	0.2973	0.5760	0.1267	S
6	0.4067	0.0425	0.5508	0.3860	0.1355	0.4785	0.2822	0.5982	0.1196	S
7	0.3769	0.0476	0.5755	0.3309	0.1725	0.4966	0.0663	0.9055	0.0282	S
8	0.3665	0.0477	0.5857	0.3176	0.1797	0.5027	0.0353	0.9496	0.0151	S
9	0.3236	0.0502	0.6262	0.2697	0.2085	0.5218				B
10	0.2894	0.0555	0.6551	0.2315	0.2452	0.5233				B
11	0.2316	0.0772	0.6912	0.1896	0.2476	0.5628				B
12	0.1865	0.1039	0.7096	0.1474	0.2972	0.5554				B
13	0.1327	0.1460	0.7213	0.1150	0.2607	0.6243				B
14	0.1037	0.1728	0.7235	0.0822	0.3474	0.5704				B
15	0.0499	0.2278	0.7223	0.0402	0.3809	0.5789				B
16	0	0.2841	0.7159							B

^aThe mass fraction of the salt. ^bThe dried solid phase means LiCl·H₂O + NH₄Cl without solution. ^cA = LiCl·H₂O, S = solid solution (NH₄Cl)_x(LiCl·H₂O)_{1-x}, B = NH₄Cl.

Table 3. Solubility of the Ternary System LiCl + NH₄Cl + H₂O at 323.15 K

no.	composition of solution ^a			composition of wet solid phase ^a			composition of dried solid phase ^b			solid phase ^c
	LiCl	NH ₄ Cl	H ₂ O	LiCl	NH ₄ Cl	H ₂ O	LiCl	NH ₄ Cl	H ₂ O	
1	0.4835	0	0.5165							A
2	0.4788	0.0117	0.5095	0.5576	0.0074	0.4350				A
3	0.4662	0.0284	0.5054	0.4813	0.1008	0.4179	0.5168	0.2627	0.2205	S
4	0.4504	0.0427	0.5069	0.4692	0.1410	0.3898	0.4951	0.2918	0.2131	S
5	0.4339	0.0550	0.5111	0.4125	0.1634	0.4241	0.3494	0.5005	0.1501	S
6	0.4036	0.0728	0.5236	0.3596	0.2698	0.3706	0.2891	0.5874	0.1235	S
7	0.3771	0.0785	0.5444	0.3088	0.2647	0.4265	0.0725	0.8953	0.0322	S
8	0.3714	0.0776	0.5510	0.3024	0.2609	0.4367	0.0570	0.9169	0.0261	S
9	0.3347	0.0800	0.5853	0.2675	0.2654	0.4671				B
10	0.2618	0.0985	0.6397	0.2203	0.2437	0.5360				B
11	0.2316	0.1138	0.6545	0.1938	0.2609	0.5453				B
12	0.1844	0.1435	0.6721	0.1377	0.3615	0.5008				B
13	0.1349	0.1877	0.6774	0.1129	0.3174	0.5697				B
14	0.0690	0.2552	0.6758	0.0557	0.4002	0.5441				B
15	0	0.3324	0.6676							B

^aThe mass fraction of the salt. ^bThe dried solid phase means LiCl·H₂O + NH₄Cl without solution. ^cA = LiCl·H₂O, S = solid solution (NH₄Cl)_x(LiCl·H₂O)_{1-x}, B = NH₄Cl.

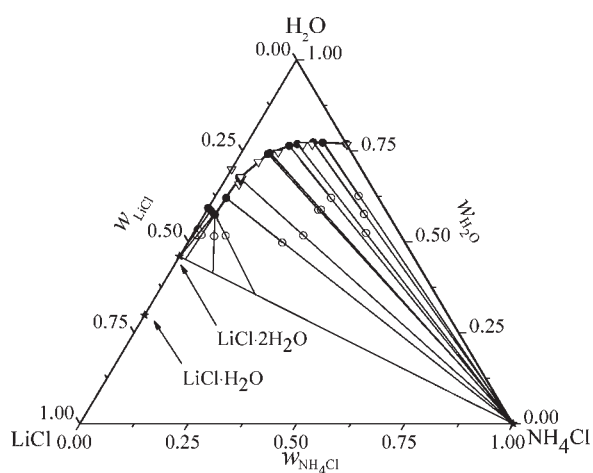


Figure 1. Isothermal solubility curve for the system LiCl + NH₄Cl + H₂O at 273.15 K. ●, saturated solution composition in this work; ○, corresponding wet solid composition in this work; ▽, ref. 3.

result⁶ $w = 0.4073$ very well. In the ternary LiCl + NH₄Cl + H₂O system our results agree with the results of Wang et al.³ on the NH₄Cl-rich side, but on the LiCl-rich side, the results of Wang et al. are obviously wrong, as shown in Figure 1.

At 298.15 K our solubility data coincide with the literature data² very well on the NH₄Cl-rich side. On the LiCl-rich side Voskresenskaya and Yanat'eva² reported that there is an invariant point for the two solid phases, LiCl·H₂O and NH₄Cl. They reported further that there are only two crystallization branches at 298.15 K. This is not true according to our results, as shown in Figure 2. In the region near the so-called invariant point found by Voskresenskaya and Yanat'eva, we found that several extension lines determined by saturated solution composition and corresponding wet solid composition do not go through the pure LiCl·H₂O or NH₄Cl composition points, and their saturated solution compositions differ from each other. According to Schreinemakers' method,

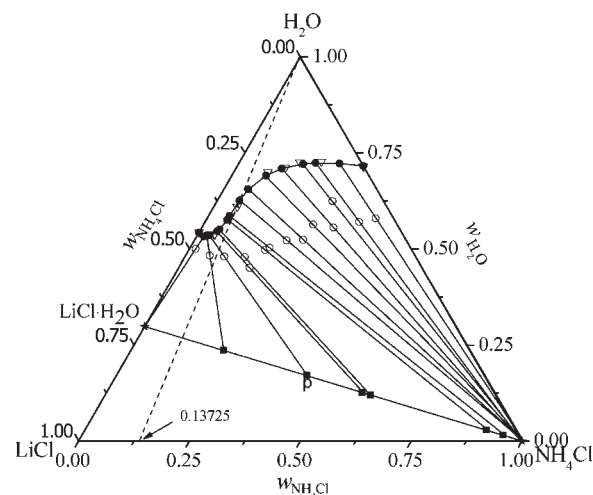


Figure 2. Isothermal solubility curve for the system LiCl + NH₄Cl + H₂O at 298.15 K. ●, saturated solution composition in this work; ○, corresponding wet solid composition in this work; ■, corresponding dried solid composition in this work; ▽, ref. 2.

the corresponding solid phase cannot be the mixture of the solid phases LiCl·H₂O and NH₄Cl. To identify the crystal type, we measured the pure LiCl·H₂O, NH₄Cl, and the dried solid phase (point p in Figure 2) by X-ray diffraction, and the obtained results are shown in Figure 4. It can be observed that the X-ray diffraction patterns for the pure solid phases LiCl·H₂O and NH₄Cl are generally similar (see Figure 4a), the characteristic peaks of the dried solids phase (point p in Figure 2) locate between that of the solid LiCl·H₂O and NH₄Cl (see Figure 4b), and thus it cannot be the simple mixture of LiCl·H₂O and NH₄Cl, but one kind of solid solution. Furthermore, we analyzed the dried solid composition as described in the Experimental Section. It was found that the dried solid composition falls on the connected line between LiCl·H₂O and NH₄Cl. The new found solid phase is expressed as (NH₄Cl)_x(LiCl·H₂O)_{1-x} later in this work.

Analogous to the case at 298.15 K, there are also three solubility branches at 323.15 K, as shown in Figure 3. One remarkable difference is that the formation region of the solid solution gets larger with increasing temperature. In the process of NH_4Cl crystallization from the $\text{LiCl} + \text{NH}_4\text{Cl}$ aqueous solution, to avoid the formation of $\text{LiCl} \cdot \text{H}_2\text{O}$ along with NH_4Cl , the salt composition in the solution should be controlled to $w_{\text{NH}_4\text{Cl}}/(w_{\text{NH}_4\text{Cl}} + w_{\text{LiCl}}) > 0.1373$ at 298.15 K and $w_{\text{NH}_4\text{Cl}}/(w_{\text{NH}_4\text{Cl}} + w_{\text{LiCl}}) > 0.1970$ at 323.15 K, respectively.

Modeling. As discussed in our previous work,⁷ the Pitzer–Simonson–Clegg model^{8–10} is a good selection to describe the properties of the titled highly soluble salt aqueous solution $\text{LiCl} + \text{NH}_4\text{Cl} + \text{H}_2\text{O}$. Meanwhile, we corrected some printing failure in the literature^{9,10} and gave the corrected formulation of the water and salt activity coefficients, as described in eqs 1 to 6 in our previous work.⁷

For a single-electrolyte solution, the Pitzer–Simonson–Clegg model^{9,10} describes the solvent activity coefficient f_1 as below:

$$\ln f_1 = 2A_x I_x^{3/2} / (1 + \rho I_x^{1/2}) - x_M x_X B_{MX} \exp(-\alpha_{MX} I_x^{1/2}) - x_M x_X B_{MX}^1 \exp(-\alpha_{MX}^1 I_x^{1/2}) + x_1^2 (W_{1,MX} + (x_1 - x_1) U_{1,MX}) + 4x_1 x_M x_X (2 - 3x_1) V_{1,MX} \quad (1)$$

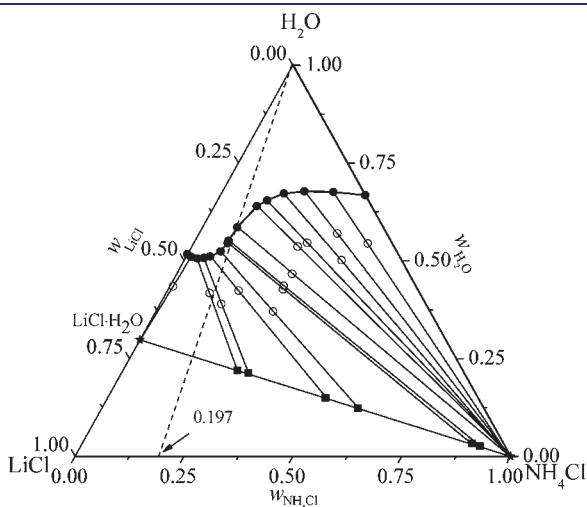


Figure 3. Isothermal solubility curve for the system $\text{LiCl} + \text{NH}_4\text{Cl} + \text{H}_2\text{O}$ at 323.15 K. All data are in this work; ●, saturated solution composition; ○, wet solid composition; ■, dried solid composition.

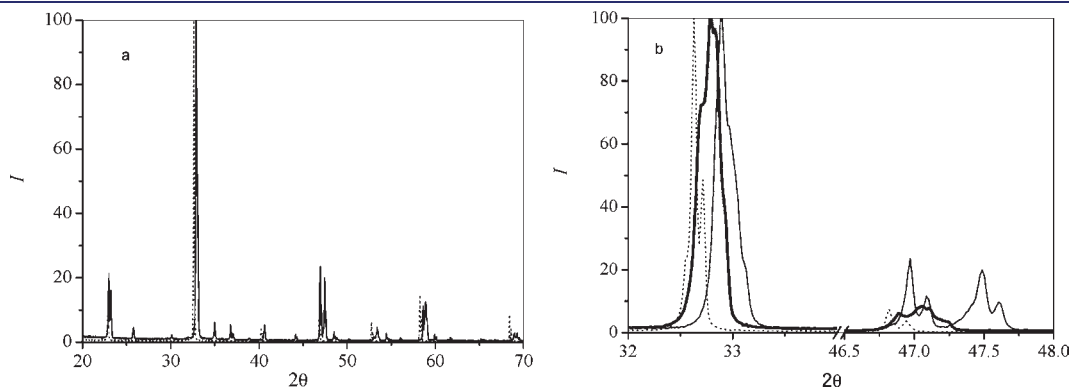


Figure 4. X-ray diffraction pattern for $\text{LiCl} \cdot \text{H}_2\text{O}$ (fine solid line), NH_4Cl (dotted line) and solid phase p in Figure 2 (thick line). I , relative intensity; 2θ , diffraction angle.

Cation M:

$$\ln f_M = -z_M^2 A_x [(2/\rho) \ln(1 + \rho I_x^{1/2}) + I_x^{1/2} (1 - 2I_x/z_M^2) / (1 + \rho I_x^{1/2})] + x_X B_{MX} g(\alpha_{MX} I_x^{1/2}) - x_M x_X B_{MX} [z_M^2 g(\alpha_{MX} I_x^{1/2}) / (2I_x) + (1 - z_M^2 / (2I_x)) \exp(-\alpha_{MX} I_x^{1/2})] + x_X B_{MX}^1 g(\alpha_{MX}^1 I_x^{1/2}) - x_M x_X B_{MX}^1 [z_M^2 g(\alpha_{MX}^1 I_x^{1/2}) / (2I_x) + (1 - z_M^2 / (2I_x)) \exp(-\alpha_{MX}^1 I_x^{1/2})] + x_1 ((z_M + z_X) / (2z_X) - x_1) W_{1,MX} + x_1 x_1 ((z_M + z_X) / z_X - 2x_1) U_{1,MX} + 4x_1^2 x_X (1 - 3x_M) V_{1,MX} - \frac{1}{2} [(z_M + z_X) / z_X] W_{1,MX} \quad (2)$$

and anion X:

$$\ln f_X = -z_X^2 A_x [(2/\rho) \ln(1 + \rho I_x^{1/2}) + I_x^{1/2} (1 - 2I_x/z_X^2) / (1 + \rho I_x^{1/2})] + x_M B_{MX} g(\alpha_{MX} I_x^{1/2}) - x_M x_X B_{MX} [z_X^2 g(\alpha_{MX} I_x^{1/2}) / (2I_x) + (1 - z_X^2 / (2I_x)) \exp(-\alpha_{MX} I_x^{1/2})] + x_M B_{MX}^1 g(\alpha_{MX}^1 I_x^{1/2}) - x_M x_X B_{MX}^1 [z_X^2 g(\alpha_{MX}^1 I_x^{1/2}) / (2I_x) + (1 - z_X^2 / (2I_x)) \exp(-\alpha_{MX}^1 I_x^{1/2})] + x_1 (((z_M + z_X) / 2z_M) - x_1) W_{1,MX} + x_1 x_1 ((z_M + z_X) / z_M - 2x_1) U_{1,MX} + 4x_1^2 x_M (1 - 3x_X) V_{1,MX} - \frac{1}{2} [(z_M + z_X) / z_M] W_{1,MX} \quad (3)$$

where $\rho = 2150(d_1/DT)^{1/2}$; $x_1 = x_M + x_X = 1 - x_1$; A_x and I_x are the Debye–Hückel parameter and ionic strength based on mole fraction; x_X , x_M , d_1 , D , and T are mole fractions of anion and cation, density of the solvent water, dielectric constant of the solvent, and thermodynamic temperature, respectively; B_{MX} , B_{MX}^1 , $B_{1,MX}$, $U_{1,MX}$, $V_{1,MX}$, α_{MX} , and α_{MX}^1 are model parameters.

For a symmetrical or unsymmetrical ternary system $\text{MX} - \text{NX} - \text{H}_2\text{O}$, one has

$$\ln f_1 = 2A_x I_x^{3/2} / (1 + \rho I_x^{1/2}) - x_M x_X B_{MX} \exp(-\alpha_{MX} I_x^{1/2}) - x_M x_X B_{MX}^1 \exp(-\alpha_{MX}^1 I_x^{1/2}) - x_N x_X B_{NX} \exp(-\alpha_{NX} I_x^{1/2}) - x_N x_X B_{NX}^1 \exp(-\alpha_{NX}^1 I_x^{1/2}) - 2x_M x_N (v_{MN} + I_x v_{MN}') + (1 - x_1) (1/F) \{E_M (z_M + z_X) / (z_M z_X) W_{1,MX} + E_N (z_N + z_X) / (z_N z_X) W_{1,NX}\} + (1 - 2x_1) x_X \{x_M (z_M + z_X)^2 / (z_M z_X) U_{1,MX} + x_N (z_N + z_X)^2 / (z_N z_X) U_{1,NX}\} + 4x_1 (2 - 3x_1) x_X (x_M V_{1,MX} + x_N V_{1,NX}) - 2x_M x_N W_{MNX} - 4x_M x_N (x_M / v_{M(X)} - x_N / v_{N(X)}) U_{MNX} + 4(1 - 2x_1) x_M x_N Q_{1,MNX} \quad (4)$$

Table 4. Binary Parameters of the Pitzer–Simonson–Clegg Model

system	binary parameters ^a										ref
	B_{mx}		W_{mx}		U_{mx}		V_{mx}		m_{max}	T	
	A	B	A	B	A	B	A	B	mol·kg ⁻¹	K	
LiCl + H ₂ O	1045.54	-2.7353	9.78	-0.0327	93.32	-0.2154	-114.26	0.2701	19	273–323	11
NH ₄ Cl + H ₂ O	56.54	-0.1517	12.28	-0.0328	37.67	-0.0926	-28.81	0.0739	7.5	273–323	12, 13

^aParameter value = $A + B(T/K)$.

$$\begin{aligned} \ln f_M = & -z_M^2 A_x [(2/\rho) \ln(1 + \rho I_x^{1/2}) + I_x^{1/2} (1 - 2I_x/z_M^2)] \\ & / (1 + \rho I_x^{1/2}) + x_X B_{MX} g(\alpha_{MX} I_x^{1/2}) + x_X B_{MX}^1 g(\alpha_{MX}^1 I_x^{1/2}) \\ & - x_M x_X B_{MX} [z_M^2 g(\alpha_{MX} I_x^{1/2}) / (2I_x) + (1 - z_M^2 / (2I_x)) \exp(-\alpha_{MX} I_x^{1/2})] \\ & - x_M x_X B_{MX}^1 [z_M^2 g(\alpha_{MX}^1 I_x^{1/2}) / (2I_x) + (1 - z_M^2 / (2I_x)) \exp(-\alpha_{MX}^1 I_x^{1/2})] \\ & - x_N x_X B_{NX} [z_M^2 g(\alpha_{NX} I_x^{1/2}) / (2I_x) + (1 - z_M^2 / (2I_x)) \exp(-\alpha_{NX} I_x^{1/2})] \\ & - x_N x_X B_{NX}^1 [z_M^2 g(\alpha_{NX}^1 I_x^{1/2}) / (2I_x) + (1 - z_M^2 / (2I_x)) \exp(-\alpha_{NX}^1 I_x^{1/2})] \\ & + 2x_N (\nu_{MN} - x_M (\nu_{MN} + \nu'_{MN} (I_x - z_M^2/2))) + x_1 [(z_M + z_X) / z_X W_{1,MX} \\ & - (z_M/2 + 1/F) (E_M (z_M + z_X) / (z_M z_X) W_{1,MX}) + E_N (z_N + z_X) \\ & / (z_N z_X) W_{1,NX}] + x_1 x_X [(z_M + z_X)^2 / (z_M z_X) U_{1,MX} - 2(x_M (z_M + z_X)^2 \\ & / (z_M z_X) U_{1,MX} + x_N (z_N + z_X)^2 / (z_N z_X) U_{1,NX})] + 4x_1^2 x_X (V_{1,MX} - 3x_M V_{1,MX} \\ & - 3x_N V_{1,NX}) + 2(x_N W_{MNX} - x_M x_N W_{MNX}) + 2[x_N (2x_M / \nu_{M(X)} \\ & - x_N / \nu_{N(X)}) U_{MNX} - 2x_M x_N (x_M / \nu_{M(X)} - x_N / \nu_{N(X)}) U_{MNX}] \\ & + 4x_1 (x_N Q_{1,MNX} - 2x_M x_N Q_{1,MNX}) - [(1 - E_M/2) (z_M + z_X) \\ & / z_X W_{1,MX} - \frac{1}{2} z_M E_N (z_N + z_X) / (z_N z_X) W_{1,NX}] \quad (5) \end{aligned}$$

$$\begin{aligned} \ln f_X = & -z_X^2 A_x [(2/\rho) \ln(1 + \rho I_x^{1/2}) + I_x^{1/2} (1 - 2I_x/z_X^2)] \\ & / (1 + \rho I_x^{1/2}) + x_M B_{MX} g(\alpha_{MX} I_x^{1/2}) + x_M B_{MX}^1 g(\alpha_{MX}^1 I_x^{1/2}) \\ & + x_N B_{NX} g(\alpha_{NX} I_x^{1/2}) + x_N B_{NX}^1 g(\alpha_{NX}^1 I_x^{1/2}) - x_M x_X B_{MX} [z_X^2 g(\alpha_{MX} I_x^{1/2}) \\ & / (2I_x) + (1 - z_X^2 / (2I_x)) \exp(-\alpha_{MX} I_x^{1/2})] - x_M x_X B_{MX}^1 [z_X^2 g(\alpha_{MX}^1 I_x^{1/2}) \\ & / (2I_x) + (1 - z_X^2 / (2I_x)) \exp(-\alpha_{MX}^1 I_x^{1/2})] - x_N x_X B_{NX} [z_X^2 g(\alpha_{NX} I_x^{1/2}) \\ & / (2I_x) + (1 - z_X^2 / (2I_x)) \exp(-\alpha_{NX} I_x^{1/2})] - x_N x_X B_{NX}^1 [z_X^2 g(\alpha_{NX}^1 I_x^{1/2}) \\ & / (2I_x) + (1 - z_X^2 / (2I_x)) \exp(-\alpha_{NX}^1 I_x^{1/2})] - 2x_M x_N (\nu_{MN} + \nu'_{MN} (I_x - z_X^2/2)) \\ & + x_1 E_M [(z_M + z_X) / z_M W_{1,MX} - (z_X/2 + 1/F) (z_M + z_X) / (z_M z_X) W_{1,MX}] \\ & + x_1 E_N [(z_N + z_X) / z_N W_{1,NX} - (z_X/2 + 1/F) (z_N + z_X) / (z_N z_X) W_{1,NX}] \\ & + x_1 x_M [(z_M + z_X)^2 / (z_M z_X) U_{1,MX} - 2(x_X (z_M + z_X)^2 / (z_M z_X) U_{1,MX}) \\ & + x_1 x_N [(z_N + z_X)^2 / (z_N z_X) U_{1,NX} - 2(x_X (z_N + z_X)^2 / (z_N z_X) U_{1,NX})] \\ & + 4x_1^2 x_M (V_{1,MX} - 3x_X V_{1,MX}) + 4x_1^2 x_N (V_{1,NX} - 3x_X V_{1,NX}) - 2x_M x_N W_{MNX} \\ & - 4x_M x_N (x_M / \nu_{M(X)} - x_N / \nu_{N(X)}) U_{MNX} - 8x_1 x_M x_N Q_{1,MNX} \\ & - \frac{1}{2} [E_M (z_M + z_X) / z_M W_{1,MX} + E_N (z_N + z_X) / z_N W_{1,NX}] \quad (6) \end{aligned}$$

where W_{MNX} , $Q_{1,MNX}$, and U_{MNX} are ternary model parameters.

The binary model parameters in eqs 1, 2, and 3 which were fitted to the experimental data^{11–13} are listed in Table 4. In eq 1, we choose the experience constant $\alpha = 13.0$, $\alpha_1 = 13.0$ as the

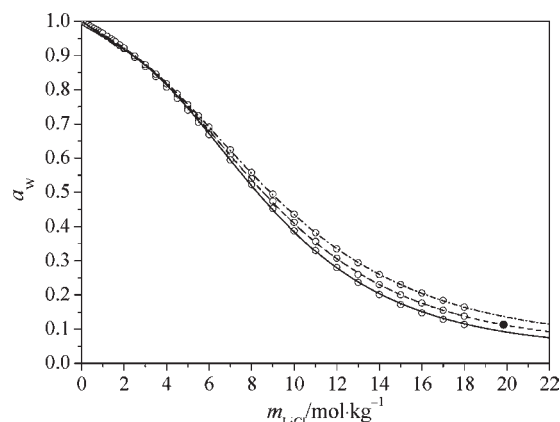
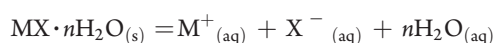


Figure 5. Calculated water activities for the system LiCl + H₂O compared with literature data. ○, ref 11; ●, ref 14; all lines are model values: —, $T = 273.15$ K; ---, $T = 298.15$ K; - · -, $T = 323.15$ K.

literature value.¹⁰ The calculated water activity curves are presented in Figures 5 and 6. The water activities in the system LiCl + H₂O predicted by the model agree with other literature data¹⁴ very well.

The $\ln k$ parameter for each solid phase is determined by calculating the component activities (eq 7) at its saturated solution¹⁵ and is listed in Table 5.



$$\ln k = \ln(a_{M^+_{(aq)}} a_{X^-_{(aq)}} a_{H_2O}^n) \quad (7)$$

The calculated liquidus of the two binary systems LiCl + H₂O and NH₄Cl + H₂O are shown in Figures 7 and 8. Naturally, they agree with the experimental data.¹⁵

Applying the binary parameters in Tables 4 and 5, we predicted the solubility isotherms of the ternary system LiCl + NH₄Cl + H₂O at (273.15, 298.15, and 323.15) K and present the predicted results in Figure 9, which deviate largely from our experimental data. Again, we calculated the water activities in the ternary system with the binary pure salt parameters only and compared them with the experimental data^{16,17} (see Figure 10 and Table 6), finding large deviations between them too. It seems that the ternary model parameters are necessary to describe the properties of the system. To simplify the fitting procedure, we fitted the parameters to the solubility isotherms at (273.15 and 323.15) K, obtaining the ternary parameters as a function of temperature (see Table 7). The solubility isotherms calculated with both binary and ternary parameters are shown in solid lines in Figure 9. Meanwhile, the predicted water activities in the

ternary system at 298.15 K agree with the experimental data;^{16,17} see Figure 10 and Table 6. The agreement of calculated and experimental data in solubility and water activity shows the thermodynamic consistence of the properties of the ternary system measured by different research groups.

Further more, the water activities in the ternary system at 298.15 K were systematically calculated; see Figure 11. It is shown that the water activities in this system are positively deviated from the addition rule and the maximal deviation arises on the NH_4Cl -rich side. The reasons resulting this phenomenon are still unknown for us. Possibly, free Cl^- ions donated by NH_4Cl strengthen the transformation $\text{Li}(\text{H}_2\text{O})_m^+ \rightarrow \text{LiCl}(\text{H}_2\text{O})_{m-n}^+$, resulting in the release of some bound water and the increase of water activities.

For the equilibrium between aqueous solution (aq) and solid solution (ss), we have

$$\begin{aligned} (\text{LiCl} \cdot \text{H}_2\text{O} + \text{NH}_4\text{Cl})_{(\text{ss})} &= \text{Li}^+_{(\text{aq})} + \text{NH}_4^+_{(\text{aq})} \\ &+ \text{X}^-_{(\text{aq})} + \text{H}_2\text{O}_{(\text{aq})} \\ \mu_{\text{LiCl} \cdot \text{H}_2\text{O}(\text{ss})} &= \mu_{\text{Li}^+_{(\text{aq})}} + \mu_{\text{Cl}^-_{(\text{aq})}} + \mu_{\text{H}_2\text{O}_{(\text{aq})}} \\ &= \mu_{\text{Li}^+_{(\text{aq})}}^\ominus + \mu_{\text{Cl}^-_{(\text{aq})}}^\ominus + \mu_{\text{H}_2\text{O}_{(\text{aq})}}^\ominus \\ &+ RT \ln(a_{\text{Li}^+_{(\text{aq})}} a_{\text{Cl}^-_{(\text{aq})}} a_{\text{H}_2\text{O}_{(\text{aq})}}) \end{aligned} \quad (8)$$

$$\begin{aligned} \mu_{\text{NH}_4\text{Cl}(\text{ss})} &= \mu_{\text{NH}_4^+_{(\text{aq})}} + \mu_{\text{Cl}^-_{(\text{aq})}} = \mu_{\text{NH}_4^+_{(\text{aq})}}^\ominus + \mu_{\text{Cl}^-_{(\text{aq})}}^\ominus \\ &+ RT \ln(a_{\text{NH}_4^+_{(\text{aq})}} a_{\text{Cl}^-_{(\text{aq})}}) \end{aligned} \quad (9)$$

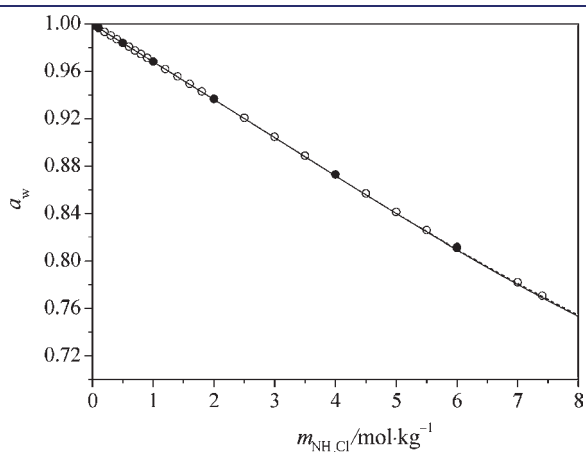


Figure 6. Calculated water activities for the system $\text{NH}_4\text{Cl} + \text{H}_2\text{O}$ compared with literature data. \circ , ref 12; \bullet , ref 13. Lines, model values: —, 298.15 K; ---, 323.15 K.

In solid solution, one has

$$\mu_{\text{LiCl} \cdot \text{H}_2\text{O}(\text{ss})} = \mu_{\text{LiCl} \cdot \text{H}_2\text{O}(\text{s})}^\ominus + RT \ln a_{\text{LiCl} \cdot \text{H}_2\text{O}(\text{ss})} \quad (10)$$

$$\mu_{\text{NH}_4\text{Cl}(\text{ss})} = \mu_{\text{NH}_4\text{Cl}(\text{s})}^\ominus + RT \ln a_{\text{NH}_4\text{Cl}(\text{ss})} \quad (11)$$

For solid–liquid equilibrium in a binary system, one has

$$\begin{aligned} \mu_{\text{LiCl} \cdot \text{H}_2\text{O}(\text{s})}^\ominus &= \mu_{\text{Li}^+_{(\text{aq})}}^\ominus + \mu_{\text{Cl}^-_{(\text{aq})}}^\ominus + \mu_{\text{H}_2\text{O}_{(\text{aq})}}^\ominus \\ &+ RT \ln(a_{\text{Li}^+_{(\text{aq})}} a_{\text{Cl}^-_{(\text{aq})}} a_{\text{H}_2\text{O}_{(\text{aq})}}) = \mu_{\text{Li}^+_{(\text{aq})}}^\ominus \\ &+ \mu_{\text{Cl}^-_{(\text{aq})}}^\ominus + \mu_{\text{H}_2\text{O}_{(\text{aq})}}^\ominus + RT \ln k_{\text{LiCl} \cdot \text{H}_2\text{O}} \end{aligned} \quad (12)$$

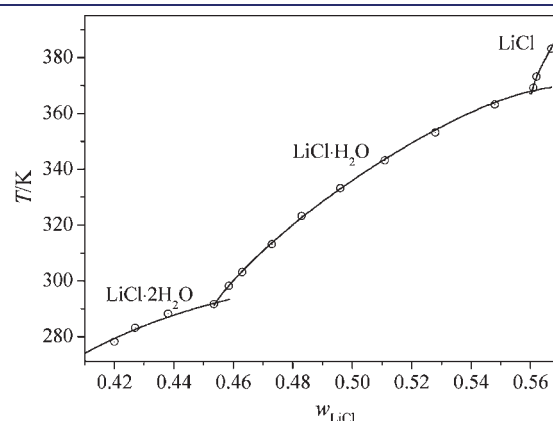


Figure 7. Calculated liquidus for the system $\text{LiCl} + \text{H}_2\text{O}$ compared with literature data. \circ , ref 15; —, model value.

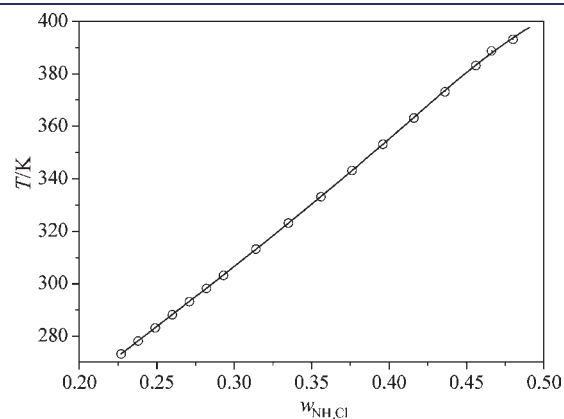


Figure 8. Calculated liquidus for the system $\text{NH}_4\text{Cl} + \text{H}_2\text{O}$ compared with the literature data. \circ , ref 15; —, model value.

Table 5. Parameter $\ln k$ of Solid Phases in the Ternary $\text{LiCl} + \text{NH}_4\text{Cl} + \text{H}_2\text{O}$ System

solid phase	$\ln k$	T/K	ref
$\text{LiCl} \cdot 2\text{H}_2\text{O}$	$\ln k = 8.06 - 0.018(T/\text{K})$	273.15—291.65	15
$\text{LiCl} \cdot \text{H}_2\text{O}$	$\ln k = -1284.11 + 34000.12(T/\text{K})$ $- 0.42(T/\text{K}) + 228.24 \ln(T/\text{K})$	291.65—369.15	15
LiCl	$\ln k = -12782.25 + 406117.22/(T/\text{K})$ $- 2.94(T/\text{K}) + 2160.71 \ln(T/\text{K})$	373.15—433.15	15
NH_4Cl	$\ln k = -378.22 + 6873.22/(T/\text{K})$ $- 0.13(T/\text{K}) + 68.35 \ln(T/\text{K})$	273.15—473.15	15

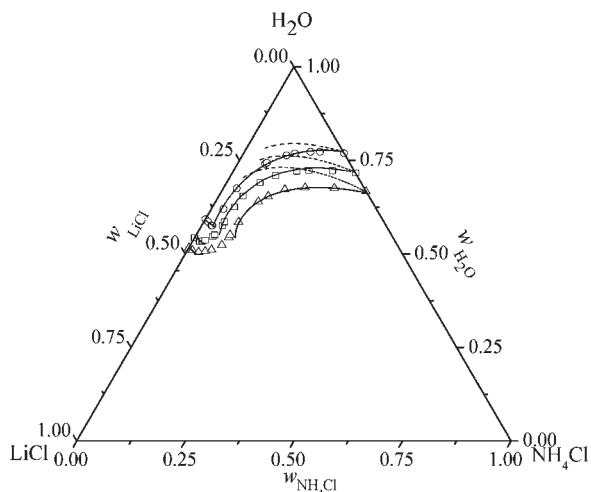


Figure 9. Isothermal solubility curve for the system LiCl + NH₄Cl + H₂O. Symbols, experimental data: ○, 273.15 K; □, 298.15 K; △, 323.15 K. ---, predicted isotherms with binary parameters only; —, predicted isotherms with both binary and ternary parameters.

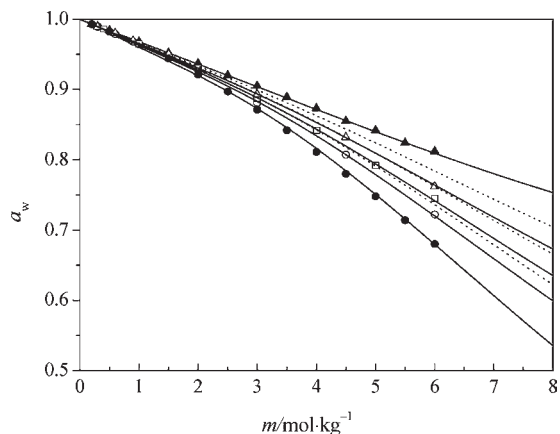


Figure 10. Calculated water activity for the system LiCl + NH₄Cl + H₂O against total m at different ionic-strength fractions y of NH₄Cl at $T = 298.15$ K. Symbols, experimental data from refs 16 and 17: ●, $y = 0$; ○, $y = 0.33$; □, $y = 0.5$; △, $y = 0.67$; ▲, $y = 1$; —, model value calculated with both binary and ternary parameters; ---, model value calculated with binary parameters only.

$$\begin{aligned}\mu_{\text{NH}_4\text{Cl}(s)}^\ominus &= \mu_{\text{NH}_4^+(\text{aq})}^\ominus + \mu_{\text{Cl}^-(\text{aq})}^\ominus + RT \ln(a_{\text{NH}_4^+(\text{aq})} a_{\text{Cl}^-(\text{aq})}) \\ &= \mu_{\text{NH}_4^+(\text{aq})}^\ominus + \mu_{\text{Cl}^-(\text{aq})}^\ominus + RT \ln k_{\text{NH}_4\text{Cl}}\end{aligned}\quad (13)$$

Substituting eqs 8 and 12 in eq 10 and eqs 9 and 13 in eq 11, respectively, one gets the activity relation of LiCl · H₂O and NH₄Cl in the solid solution with that in aqueous solution, respectively:

$$a_{\text{LiCl}\cdot\text{H}_2\text{O}(ss)} = a_{\text{Li}^+(\text{aq})} a_{\text{Cl}^-(\text{aq})} a_{\text{H}_2\text{O}(\text{aq})} / k_{\text{LiCl}\cdot\text{H}_2\text{O}} \quad (14)$$

$$a_{\text{NH}_4\text{Cl}(ss)} = a_{\text{NH}_4^+(\text{aq})} a_{\text{Cl}^-(\text{aq})} / k_{\text{NH}_4\text{Cl}} \quad (15)$$

If we assume the solid solution to be an ideal mixture, namely, $a_{\text{LiCl}\cdot\text{H}_2\text{O}(ss)} = x_{\text{LiCl}\cdot\text{H}_2\text{O}(ss)}$ and $a_{\text{NH}_4\text{Cl}(ss)} = x_{\text{NH}_4\text{Cl}(ss)}$, then we have

$$a_{\text{LiCl}\cdot\text{H}_2\text{O}(ss)} + a_{\text{NH}_4\text{Cl}(ss)} = x_{\text{LiCl}\cdot\text{H}_2\text{O}(ss)} + x_{\text{NH}_4\text{Cl}(ss)} \quad (16)$$

Table 6. Comparison of Experimental and Calculated Water Activities in the Ternary System LiCl + NH₄Cl + H₂O at 298.15 K^a

$m/\text{mol}\cdot\text{kg}^{-1}$		a_w			deviation	
LiCl	NH ₄ Cl	exp ¹⁷	calc1	calc2	delta1	delta2
0.2	0.1	0.990	0.9890	0.9890	-0.0010	-0.0010
0.4	0.2	0.979	0.9776	0.9778	-0.0014	-0.0012
0.6	0.3	0.968	0.9664	0.9669	-0.0016	-0.0011
1.0	0.5	0.947	0.9442	0.9456	-0.0028	-0.0014
2.0	1.0	0.881	0.8831	0.8881	0.0021	0.0071
3.0	1.5	0.807	0.8178	0.8075	0.0108	0.0005
4.0	2.0	0.722	0.7365	0.7204	0.0145	-0.0016
0.2	0.2	0.986	0.9856	0.9857	-0.0004	-0.0003
0.5	0.5	0.965	0.9641	0.9647	-0.0009	-0.0003
1.0	1.0	0.93	0.9279	0.9306	-0.0021	0.0006
1.5	1.5	0.887	0.8943	0.8883	0.0073	0.0013
2.0	2.0	0.842	0.8537	0.8435	0.0117	0.0015
2.5	2.5	0.792	0.8092	0.7912	0.0172	-0.0008
3.0	3.0	0.745	0.7620	0.7417	0.0170	-0.0033
0.1	0.2	0.989	0.9896	0.9896	0.0006	0.0006
0.2	0.4	0.98	0.9791	0.9794	-0.0009	-0.0006
0.3	0.6	0.969	0.9688	0.9693	-0.0002	0.0003
0.5	1.0	0.95	0.9482	0.9496	-0.0018	-0.0004
1.0	2.0	0.893	0.8991	0.8935	0.0061	0.0005
1.5	3.0	0.832	0.8434	0.8313	0.0114	-0.0007
2.0	4.0	0.762	0.7837	0.7636	0.0217	0.0016
average					0.0064	0.0013

^a calc1: calculated by the binary pure solution parameters only; calc2: calculated with both binary and ternary parameters; delta1 = $a_w(\text{calc1}) - a_w(\text{exp})$; delta2 = $a_w(\text{calc2}) - a_w(\text{exp})$. average = $\sum_i^x (|\text{delta}_i|/n)$.

Substituting eqs 14 and 15 in eq 16, one gets

$$a_{\text{Li}^+(\text{aq})} a_{\text{Cl}^-(\text{aq})} a_{\text{H}_2\text{O}(\text{aq})} / k_{\text{LiCl}\cdot\text{H}_2\text{O}} + a_{\text{NH}_4^+(\text{aq})} a_{\text{Cl}^-(\text{aq})} / k_{\text{NH}_4\text{Cl}} = 1 \quad (17)$$

Using eq 17 as criterion, one can obtain the liquidus in equilibrium with the assumed ideal solid solution, as shown in dotted lines in Figure 12. The dotted lines are different from the experimental liquidus for the solid solution.

When we assume that the solid solution is a regular solution, then we have

$$a_{\text{LiCl}\cdot\text{H}_2\text{O}(ss)} = x_{\text{LiCl}\cdot\text{H}_2\text{O}(ss)} \exp(\Omega x_{\text{NH}_4\text{Cl}}^2 / RT) \quad (18)$$

$$a_{\text{NH}_4\text{Cl}(ss)} = x_{\text{NH}_4\text{Cl}(ss)} \exp(\Omega x_{\text{LiCl}\cdot\text{H}_2\text{O}}^2 / RT) \quad (19)$$

Substituting eqs 18 and 19 in eqs 14 and 15, respectively, and combining the resulted equations, one has

$$\begin{aligned}a_{\text{Li}^+(\text{aq})} a_{\text{Cl}^-(\text{aq})} a_{\text{H}_2\text{O}(\text{aq})} / (k_{\text{LiCl}\cdot\text{H}_2\text{O}} \exp(\Omega x_{\text{NH}_4\text{Cl}}^2 / RT)) \\ + a_{\text{NH}_4^+(\text{aq})} a_{\text{Cl}^-(\text{aq})} / (k_{\text{NH}_4\text{Cl}} \exp(\Omega x_{\text{LiCl}\cdot\text{H}_2\text{O}}^2 / RT)) \\ = x_{\text{LiCl}\cdot\text{H}_2\text{O}(ss)} + x_{\text{NH}_4\text{Cl}(ss)} = 1\end{aligned}\quad (20)$$

Fitting eq 20 to the experimental liquidus for solid solution, we get $\Omega = 1000 \text{ J}\cdot\text{mol}^{-1}$ and the calculated liquidus for the solid solution is shown in the dashed lines in Figure 12. The calculated liquidus represents successfully the liquidus for solid solution at 298.15 K but however fails at 323.15 K. When the solid solution is assumed to be quasi-regular solution, the fittings fail still.

Table 7. Mixture Model Parameters of the Pitzer–Simonson–Clegg Model

system	mixture parameters ^a						T/K
	W_{mnx}		Q_{mnx}		U_{mnx}		
	A	B	A	B	A	B	
LiCl + NH ₄ Cl + H ₂ O	-5.24	-0.021	-3.50	0.024	47.24	-0.14	273.15–323.15

^aParameter value = A + B(T/K).

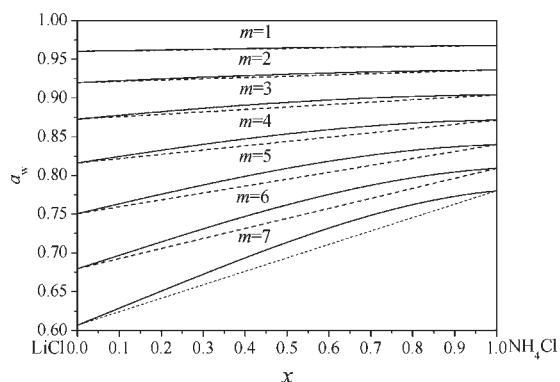


Figure 11. Deviation of water activity from the addition rule in the solution $\{(1 - x) \text{ mol LiCl} + x \text{ mol NH}_4\text{Cl} + 55.508 \text{ mol H}_2\text{O}\}$ at 298.15 K.

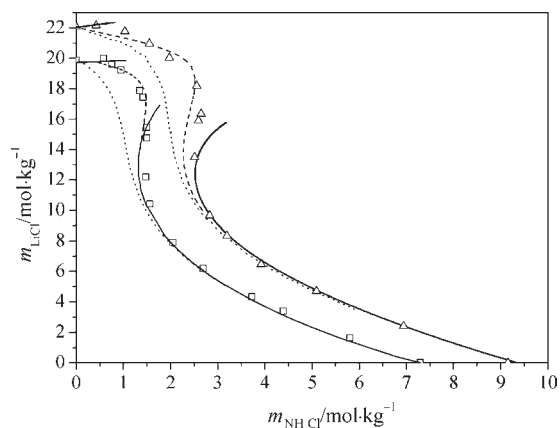


Figure 12. Solubility isotherm curve for the system LiCl + NH₄Cl + H₂O. Symbols, experimental data in this work. □ (298.15 K) and △ (323.15 K) for NH₄Cl; ■ (298.15 K) and ▲ (323.15 K) for LiCl·H₂O; □ (half filled, 298.15 K) and △ (half filled, 323.15 K) for solid solution; dotted lines, predicted assuming the solid solution as ideal solution, dashed lines, calculated assuming the solid solution as regular solution with $\Omega = 1000 \text{ J} \cdot \text{mol}^{-1}$.

CONCLUSIONS

The solubility isotherms of the system LiCl + NH₄Cl + H₂O at $T = (273.15, 298.15, \text{ and } 323.15) \text{ K}$ were elaborately measured with an accuracy of 0.002 in mass fraction. It was found that there are two crystallization branches for LiCl·2H₂O and NH₄Cl at 273.15 K, but not LiCl·H₂O and NH₄Cl as reported by literature.³ A new formation branch of solid solution phase $(\text{NH}_4\text{Cl})_x(\text{LiCl} \cdot \text{H}_2\text{O})_{1-x}$ was found besides the two phases LiCl·H₂O and NH₄Cl at 298.15 K; thus, unlike that reported by literature,² there is no invariant point between LiCl·H₂O and

NH₄Cl. The formation region of the solid solution phase gets larger with increasing temperature. A Pitzer–Simonson–Clegg model was used to correlate the solubility data determined in this work and water activities reported by literature,¹⁷ and good thermodynamic consistence between them supports the reliabilities of these data. A regular solution was assumed for the solid solution to correlate its equilibrium with aqueous solution, and its applicability was discussed.

AUTHOR INFORMATION

Corresponding Author

*E-mail: dewen_zeng@hotmail.com.

Funding Sources

This work was financially supported by the 100 top talents project of the Chinese Academy of Sciences.

REFERENCES

- Xu, H.; Xu, L. Separating Technique for Magnesium and Lithium from High Mg/Li Ratio Salt Lake Brine. *J. Cent. South Univ. (Sci. Technol.)* **2009**, *40*, 36–40.
- Voskresenskaya, N. K.; Yanat'eva, O. K. Equilibria in the System: Water-Lithium Chloride-Ammonium Chloride. *Izv. Sekt. Fiz.-Khim. Anal.* **1936**, *9*, 291–293.
- Wang, Z. Y.; He, Y. H.; Nie, F. The Equilibrium of the Ternary System LiCl–NH₄Cl–H₂O (0 °C, 30 °C). *J. Hanzhong Teachers College* **2003**, *21*, 64–67.
- Zeng, D. W.; Zhou, J. Thermodynamic Consistency of the Solubility and Vapor Pressure of a Binary Saturated Salt + Water System. 1. LiCl + H₂O. *J. Chem. Eng. Data* **2006**, *51*, 315–321.
- Kolthoff, M.; Sandell, E. B.; Meehan, E. J. *Quantitative Chemical Analysis*; Macmillan: New York, 1969.
- Zeng, D. W.; Ming, J. W.; Voigt, W. Thermodynamic Study of the System (LiCl + LiNO₃ + H₂O). *J. Chem. Thermodyn.* **2008**, *40*, 232–239.
- Zeng, D. W.; Wu, D. Z.; Yao, Y.; Han, H. J. Isopiestic Determination of Water Activity on the System LiNO₃–KNO₃–H₂O at 0 and 25 °C. *J. Solution Chem.* **2010**, *39*, 1360–1376.
- Pitzer, K. S.; Simonson, J. M. Thermodynamics of Multicomponent, Miscible, Ionic Systems: Theory and Equations. *J. Phys. Chem.* **1986**, *90*, 3005–3009.
- Clegg, S. L.; Pitzer, K. S. Thermodynamics of Multicomponent, Miscible, Ionic Solutions. Generalized Equations for Symmetrical Electrolytes. *J. Phys. Chem.* **1992**, *96*, 3513–3520.
- Clegg, S. L.; Pitzer, K. S.; Brimblecombe, P. Thermodynamics of Multicomponent, Miscible, Ionic Solutions. 2. Mixture Including Unsymmetrical Electrolytes. *J. Phys. Chem.* **1992**, *96*, 9470–9479.
- Gibbard, H. F.; Scatchard, J. G. Liquid-Vapor Equilibrium of Aqueous Lithium Chloride, from 25 °C to 100 °C and from 1.0 to 18.5 Molality, and Related Properties. *J. Chem. Eng. Data* **1973**, *18*, 293–298.
- Walter, J. H.; Yung, C. Osmotic Coefficients and Mean Activity Coefficients of Uni-univalent Electrolytes in Water at 25 °C. *J. Phys. Chem. Ref. Data* **1972**, *1*, 1085.

(13) Thiessen, W. E.; Simonson, J. M. Enthalpy of Dilution and the Thermodynamics of $\text{NH}_4\text{Cl}(\text{aq})$ to 523 K and 35 MPa. *J. Phys. Chem.* **1990**, *94*, 7794–7800.

(14) Yao, Y.; Sun, B.; Song, P. S.; et al. Thermodynamics of Aqueous Electrolyte Solution Isopiestic Determination of Osmotic and Activity Coefficients in $\text{LiCl-MgCl}_2\text{-H}_2\text{O}$ at 25 °C. *Acta Chim. Sin.* **1992**, *50*, 839–848.

(15) Linke, W. F.; Seidell, A. *Solubilities: Inorganic and Metal–Organic Compounds*, 4th ed.; American Chemical Society: Washington, DC, 1965.

(16) El Guendouzi, M.; Dinane, A.; Mounir, A. Water Activities, Osmotic and Activity Coefficients in Aqueous Chloride Solutions at $T = 298.15$ K by the Hygrometric Method. *J. Chem. Thermodyn.* **2001**, *33*, 1059–1072.

(17) El Guendouzi, M.; Dinane, A.; Mounir, A. Hygrometric Determination of Water Activities and Osmotic and Activity Coefficients of $\text{NH}_4\text{Cl-LiCl-H}_2\text{O}$ at 25 °C. *J. Solution Chem.* **2002**, *31*, 119–129.